

A Novel Amplitude Modulated Triangular Carrier Gain Linearization Technique for SPWM Inverter

Subburam Ramkumar¹, Seenithangam Jeevananthan²,
Vijayarajan Kamaraj³

Abstract: This paper presents a new method to extend the linearity of the sinusoidal pulse width modulation (SPWM) to full range of the pulse dropping region. The proposed amplitude modulated triangular carrier PWM method (AMTCPWM) increases the dynamic range of the SPWM control and eliminates the need of nonlinear modulation in the pulse dropping region to reach the square wave boundary. The novel method combines the spectral quality of SPWM with the efficient single-mode linear control. A simple analytical characterization of the exact method is presented and its effectiveness is demonstrated using simulation for the basic single-phase H-bridge inverter circuit. The hardware results of the designed prototype inverter are presented to validate the betterment of the novel scheme.

Keywords: PWM inverter, Overmodulation, Voltage gain linearization, Amplitude modulated carrier.

1 Introduction

Pulse width-modulated (PWM) voltage-source inverters (VSI) are widely utilized in ac motor drive applications and at a smaller quantity in controlled rectifier applications as a means of dc to ac power conversion devices (K. Udhayakumar, 2008). Utilizing the conventional VSI structure shown in Fig. 1, which consists of two switching poles, S_1/S_2 and S_3/S_4 , the appropriate carrier-based PWM method programs a “per carrier cycle average output voltage” equal to the reference voltage. The generation of PWM patterns through modulation is just amplitude to width transformation. Employing the triangle-intersection technique (I. Batarseh, 2004; S. Jeevananthan, 2007) or direct digital pulse programming technique (S. Bolognani, 1996; M. Bounadja, 2007), PWM methods provide a linear relationship between the reference and the output voltages within a limited range.

¹Professor in EEE, Surya College of Engineering & Technology, Vikiravandi 605652. India; E-mail: ramme04@gmail.com

²Pondicherry Engineering College, Pondicherry – 605 101. India, E-mail: drsj_eee@pec.edu

³SSN College of Engineering, Kalavakkam- 603 110. India; E-mail: kamarajv@ssn.edu.in

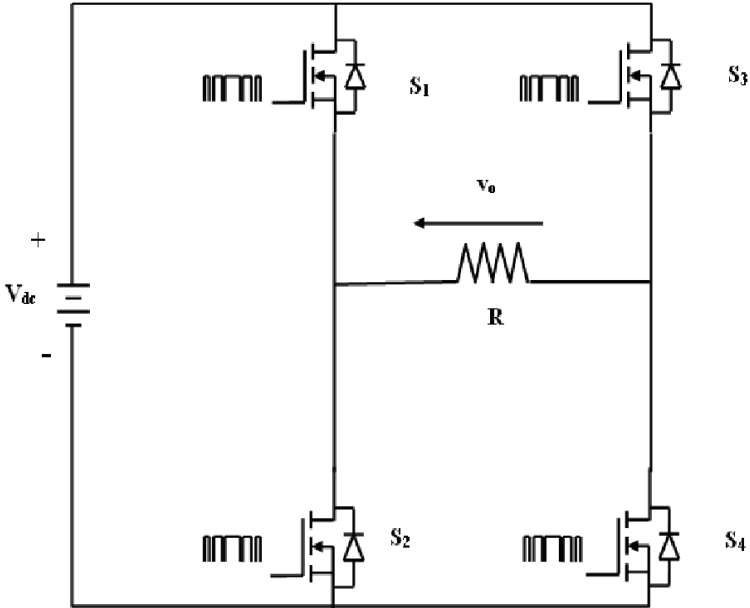


Fig. 1 – Basic single-phase inverter power circuit.

Test results from commercially available volts per hertz (V/f) drives reveal their inability to provide rated (output) voltage even at rated input voltage (V_{dc}). The higher output ranges and hence effective utilization of dc input voltage is possible by increasing the inverter modulation index more than unity (overmodulation) at the cost of reduced (nonlinear) gain. The linear modulation range harmonics of carrier-based PWM methods (characteristic harmonics) are concentrated at the carrier frequency as its sidebands. In the overmodulation region, as the unmodulated segment of the modulation wave increases, the characteristic harmonics decrease. However, large amounts of sub-carrier frequency harmonics (5th, 7th, etc.) are generated, and as the square wave mode is approached, these harmonics become increasingly dominant in determining the waveform quality (Boost M.A, 1998). The reduction of gain in the pulse dropping region restricts the range of speed and torque regulation in motor control applications (Giovanni, G, 1993). For utility interface applications as voltage source converter, it restricts the range of fluctuations in the utility voltage which can be handled effectively with low harmonic distortion. For maximum utilization of the dc bus, the PWM algorithm must balance a given/desired dc voltage on one side of the power converter with the maximum possible desired/given fundamental ac voltage on the other side of the power converter in a linear manner to square wave mode of operation (Hava, A.M, 1998).

In the case of current regulated PWM (CRPWM) inverters, the pulse dropping region demonstrates significant problems for the control engineer (J. Holtz, 1992; A.M. Hava, 1998). Other investigators have also observed the importance of designing a controller that transitions smoothly from PWM control to six-step operation (S. Bolognani, 1996; J. Holtz, 1992). Griva *et al.* like Holtz, proposed a technique by which switching times are calculated for the overmodulation region (G. Giovanni, 1993). While Holtz's technique completes the transition to six-step, Griva's method does not fully transit to six-step operation. In isolated neutral-type loads, the freedom to add a zero-sequence signal to the modulation waves leads to a large variety of modulation waves, hence modulation methods (M.A. Boost, 1998). The third harmonic injection PWM (THIPWM) technique to increase the amplitude of the fundamental component was proposed (J.A. Houldsworth, 1984), where a third harmonic wave is added to the three-phase sinusoidal modulating waves. A modified carrier PWM (MCPWM) switching strategy has been developed to achieve overmodulated fundamental voltage values with modulation depths in the linear range (S. Jeevananthan, 2005). A method to extend the linearity of the sinusoidal PWM (SPWM) is presented (R.J. Kerkman, 1994). A compensated modulation technique (CMT) adaptable to continuous and discontinuous modulators, provides the exact inverse of the nonlinearity, has been developed.

Finally, the pulse dropping region in the SPWM methods is becoming a topic of considerable interest. Though the overmodulation is unavoidable solution to the effective utilization of the input voltage, a PWM control with linear voltage gain is needed obviously, which should be also suitable for feedback controls. This paper studies conventional SPWM for voltage gain and output spectral characteristics and compares with the proposed amplitude modulated triangular PWM (AMTCPWM). The AMTCPWM method is a simple gain linearization technique based on a novel carrier function, which provides modulator linearity up to the square wave mode.

2 Review of PWM Methods

The inverter's characteristics play a significant role in establishing the performance of an ac drive. The V/f market requires a PWM algorithm that delivers the desired fundamental voltage to the motor and ensures stable operation. In addition, the performance improvement of the drive depends on the characteristics of the PWM algorithm. For example, the effort spent on selective harmonic elimination (SHE) is wasted if the adverse effects of dead time (blanking time) are not corrected. All PWM waveforms presented in this paper are assumed to be synchronous unipolar PWM voltage switching.

A Sinusoidal Pulse Width Modulation (SPWM)

The unipolar PWM pulse generation with resulting pattern is represented in Fig. 2. The harmonics present in the quasi-square wave and their relative amplitudes always remain the same. With PWM, however, the relative amplitudes of the harmonics change with the modulation index, M_a . It is generally accepted that the performance of an inverter with any switching strategy can be related to the harmonic content of its output voltage (S. Jeevananthan, 2005). A precise value of the switching angle and hence duty cycle can be obtained through the triangular (carrier) and the sinusoidal (reference) equations. The modulation pattern of the SPWM control (Fig. 2) indicates the switching angles ($p_1, p_2, p_3, \dots, p_i$). The PWM control signal is obtained by comparing a high frequency triangular carrier of frequency, f_c and amplitude 1 (per unit) and a low frequency sine wave of frequency, f_m and amplitude M_a (perunit). Equations for sinusoidal reference and triangular carrier are given by (1) and (2) respectively.

$$y = M_a \sin x, \quad (1)$$

$$x \pm \left(\frac{\pi}{2M_f} \right) y = \frac{r\pi}{M_f}. \quad (2)$$

Where, r is equal to 1 for first pair of triangular sections (straight lines), 3 for second pair; 5 for third pair and so on. '+' sign should be taken for odd numbered line sections and '-' sign for even numbered line sections. The equations describing the natural sampled switching angles are transcendental and have the general distinct solutions for odd and even switching angles. The condition for any i -th switching angles, p_i is given in (3) and (4) respectively for odd and even switching angles.

$$M_a \sin x + \frac{2M_f x}{\pi} - 2i = 0 \quad i = 1, 3, 5... \quad (3)$$

$$M_a \sin x - \frac{2M_f x}{\pi} - 2i = 0 \quad i = 2, 4, 6... \quad (4)$$

The duty cycle can be calculated by simply adding the width of the individual pulses. The pulse width, total on time and the duty cycles are represented by (5), (6) and (7) respectively. Since the inverter output irrespective of control methods exhibits equal positive and negative half cycles, which results in zero dc component ($a_0 = 0$), and also does not possess any even harmonics due to half wave symmetry. Equation (8) gives the generalized Fourier coefficients for the problem considered.

Width of the j -th pulse is:

$$W_j = P_{i+1} - P_i, \quad (5)$$

$$T_{on} = \sum_{j=1}^n \left(\left[x - \frac{\pi}{2M_f} M_a \sin x - \frac{2j}{2M_f} \right] - \left[x + \frac{\pi}{2M_f} M_a \sin x - \frac{2j}{2M_f} \right] \right). \quad (6)$$

Duty cycle is:

$$D = \frac{M_a}{M_f} \sum_{i=1}^{M_f-1} \sin \frac{i\pi}{M_f}, \quad (7)$$

$$a_n = \frac{V_{dc}}{n\pi\sqrt{2}} \sum_{k=1}^{i-1} \{ (\sin np_{k+1} - \sin np_k) - (\sin np_{k+1} - \sin np_k) \},$$

$$b_n = \frac{V_{dc}}{n\pi\sqrt{2}} \sum_{k=1}^{i-1} \{ (\cos np_{k+1} - \cos np_k) - (\cos np_{k+1} - \sin np_k) \}, \quad (8)$$

$$C_n = \sqrt{a_n^2 + b_n^2}.$$

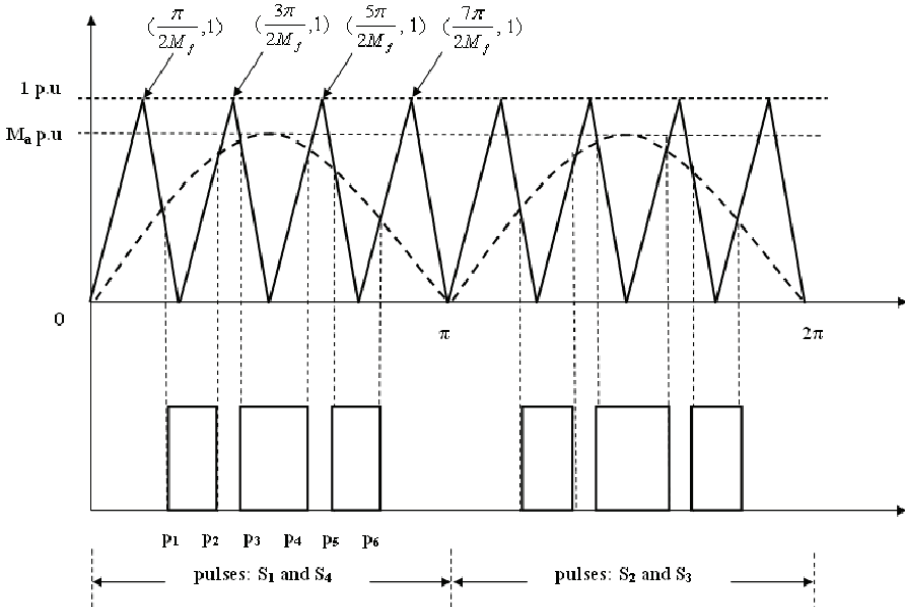


Fig. 2 – Sinusoidal pulse width modulation.

B Overmodulation

The characteristics of the SPWM and its three modes of operation are well known as shown in the Fig. 3, which is the normalized peak amplitude of

fundamental frequency component as a function of the modulation index (M.P. Kazmierkowski, 2002; I. Batarseh, 2004). In the linear mode, where the value of M_a is less than unity, the amplitude of the fundamental-frequency voltage varies linearly with M_a , and pushes the harmonics into a high-frequency range around the switching frequency and its multiples. For the increased fundamental component (more than which is achievable with linear mode), the reference command peak exceeds the peak of the carrier and the nonlinear (pulse dropping) mode starts. Operating in the nonlinear modulation range, or in more common terms, the overmodulation range is problematic:

- (i) large amounts of sub-carrier frequency harmonic currents are generated;
- (ii) the fundamental component voltage gain significantly decreases;
- (iii) the switching device gate pulses are unexpectedly dropped.

In constant V/f - controlled PWM-VSI induction motor drives, operation in this range results in poor performance and also leads in over current fault. In current-controlled drives, the current regulators are heavily burdened by the feedback current sub-carrier frequency harmonics and regulator saturation and oscillatory operations result in performance degradation. At $M_a = 3.24$ the square wave mode starts.

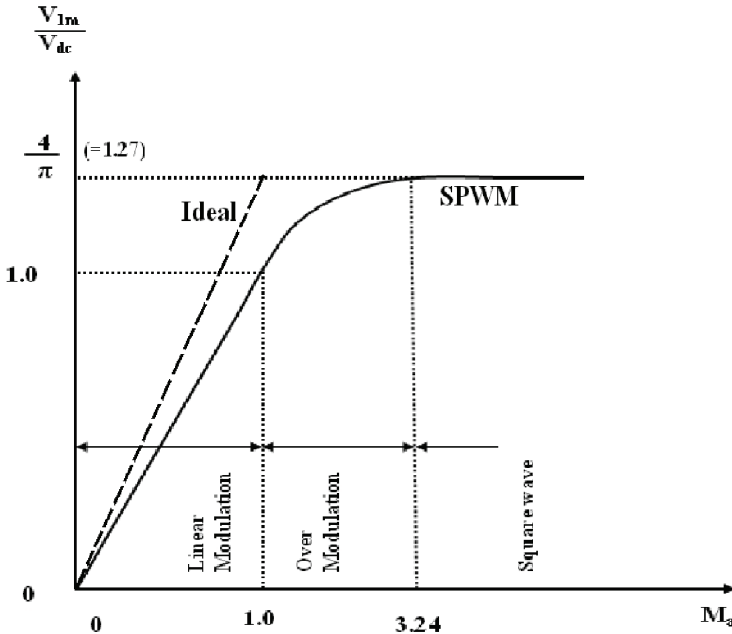


Fig. 3 – Output fundamental- M_a characteristics- SPWM and Ideal.

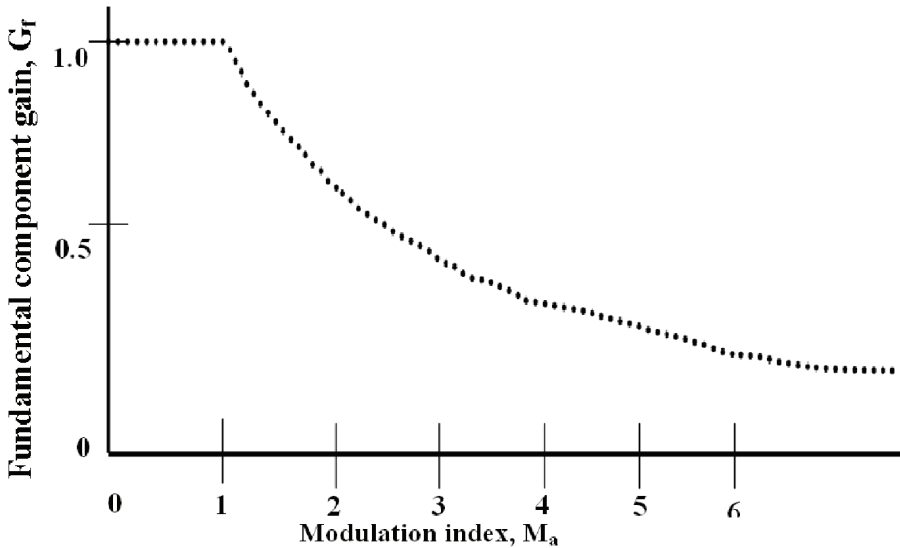


Fig. 4 – Variation of fundamental component gain with M_a .

Fig. 3 also shows the ideal fundamental component versus modulation index, M_a characteristics. Fig. 4 shows the fundamental component gain versus modulation index, M_a . For the modulation index ($M_a \leq 1$), the SPWM gain (G_f) remains constant. When the modulation index is greater than unity and the gain reduces sharply in a nonlinear manner. When the modulation index approaches very large values the gain approaches zero. Retaining the linearity until the square wave output limit is the ideal characteristics and also the requirements of feedback controllers. The existing solutions to overmodulation suffer due to the nonlinearities in the transition region. They are either very complex or demand nonlinear inverse gain calculation which results considerable amount of error and also suitable only for three-phase system. No simple PWM algorithm which retains voltage gain linearity until the full utilization of dc input for single-phase inverter system is found in the literature.

3 Proposed Amplitude Modulated Inverted Sine Wave

The purpose of this paper is to propose a modified SPWM control scheme, which offers linear gain characteristics in comparison to the conventional SPWM without involving complex computations and significant changes in device losses. The amplitude modulated triangular carrier PWM (AMTCPWM) is developed to give single mode operation of SPWM inverter by linearly hopping to square wave region. In the proposed AMTCPWM method, the conventional sine wave is reference signal and the carrier is amplitude

modulated triangular signal as shown in Fig. 5. The novel carrier is basically a high frequency triangular wave, which is (amplitude) modulated by a sinusoidal modulating signal of reference frequency.

For the AMTCPWM pulse pattern, the switching angles may be computed as the same way as SPWM scheme through analytical relations. The conditions for odd and even switching angles are given in equation (9) and the switching angles ($q_1, q_2, q_3, \dots, q_i$) are indicated in the Fig. 5. It is worth while to note that both in SPWM and AMTCPWM schemes, the number of pulses will be equal to $(M_f - 1)$ and hence the same switching loss is guaranteed (S. Jeevananthan, 2005). The modulation index for the AMTCPWM (M_t) is defined as the ratio between the amplitudes of the reference sine wave and modulating sine of triangular carrier.

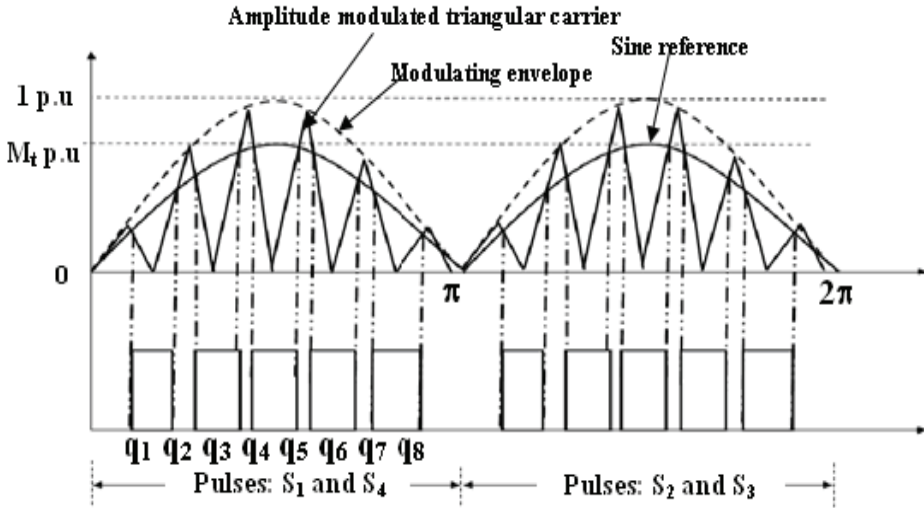


Fig. 5 – Proposed AMTCPWM.

$$M_a \sin x_i + 2 \sin \left(\frac{i\pi}{2M_f} \right) \cdot \left[\left(\frac{M_f}{\pi} \right) - \left(\frac{i+1}{2} \right) \right] = 0 \quad \text{for } i = 1, 3, 5, \dots \quad (9)$$

$$M_a \sin x_i + 2 \sin \left(\frac{(i+1)\pi}{2M_f} \right) \cdot \left[\left(\frac{i}{2} \right) - \left(\frac{M_f x_i}{\pi} \right) \right] = 0 \quad \text{for } i = 2, 4, 6, \dots$$

4 Discussion

Detailed comparison of the proposed method with conventional SPWM is presented in this chapter. It is valuable to note that the square wave operation

gives 381.97V (peak) of fundamental voltage (when $V_{dc} = 300\text{ V}$), which is 1.27 times the maximum voltage obtained in SPWM linear range. Fig. 6a and 6b show the output voltages and corresponding spectrums of SPWM for $M_f = 15$ and $V_{dc} = 300\text{ V}$ at M_a values of 0.8 and 1 respectively. In case of SPWM, the harmonics with dominant amplitudes in the linear range may not be dominant in overmodulation region. Even in linear modulation region, referring the Fig. 6a and 6b, it is understood that $M_a = 0.8$ shows the dominant inner sideband frequencies while $M_a = 1$ exhibits outer side band frequencies as dominant. Fig. 7a and 7b show output voltage and corresponding spectrum for AMTCPWM at $M_t = 0.8$ and $M_t = 0.98$. From the figures it is clear that the proposed scheme renders proportionate variation of harmonic profile unlike SPWM and hence unique filter design.

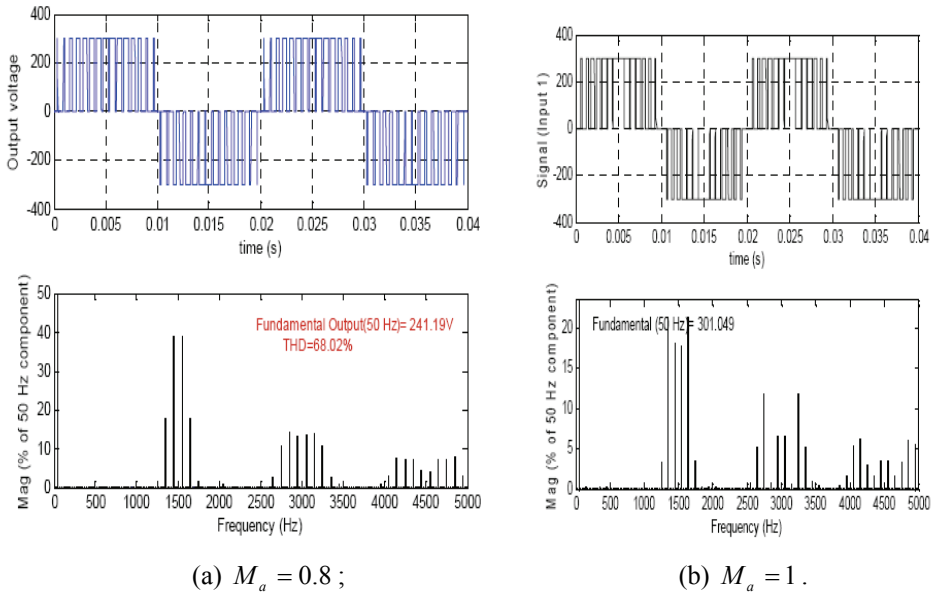


Fig. 6 – Output voltage and spectrum – SPWM.

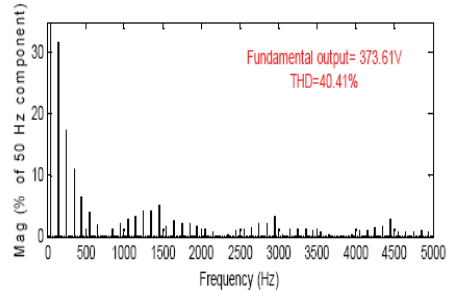
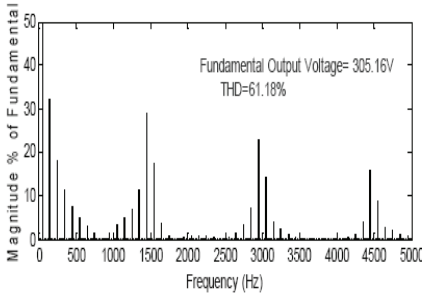
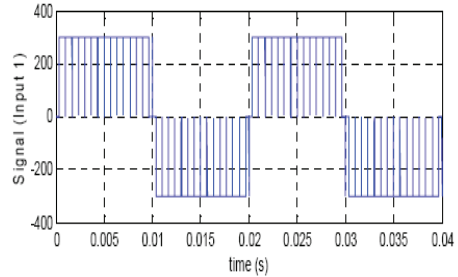
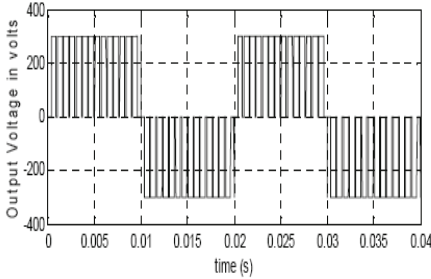
Table 1

Comparison of SPWM and AMTCPWM-sub-carrier harmonics and THD.

Method	M_a	THD [%]	h_3 [%]	h_5 [%]	h_7 [%]	h_9 [%]
SPMW	0.800	68.02	0.70	0.17	0.27	0.29
AMTCPWM	0.628	86.68	32.46	18.63	12.28	8.78

Table 2
Comparison of SPWM and AMTCPWM-carrier frequency harmonics.

Method	$2M_f - 3$	$2M_f - 1$	$2M_f + 1$	$2M_f + 3$	$4M_f - 3$	$4M_f - 1$	$4M_f + 1$	$4M_f + 3$
	h_{27} [%]	h_{29} [%]	h_{31} [%]	h_{33} [%]	h_{57} [%]	h_{59} [%]	h_{61} [%]	h_{63} [%]
SPWM	17.50	39.14	39.08	17.76	14.12	13.43	13.21	13.97
AMTCPWM	18.88	55.50	36.42	9.63	6.18	22.92	13.21	4.02



(a) $M_t = 0.8$;

(b) $M_t = 0.98$.

Fig. 7 – Output voltage spectrum – AMTCPWM.

Fig. 8 shows the variation of fundamental output voltage for various values of M_t and confirms the gain linearization property of the proposed scheme. Fig. 9 shows the THD values for entire range output voltage and the AMTCPWM exhibits higher THD than the conventional SPWM. The difference in THD between the SPWM and AMTCPWM methods are almost constant approximately equal to 20%. **Table 1** gives the values of modulation index, THD and lower order (sub-carrier) harmonics at the output voltage (peak) of 240V in both SPWM and AMTCPWM methods with 300V input and $M_f = 15$. From the table, it is understood that all the lower order harmonics are increased considerably in case of AMTCPWM method. **Table 2** presents the comparison of carrier frequency harmonics; the AMTCPWM shows always suppressed upper side band harmonics. Hence the AMTCPWM successfully extends the linearity of SPWM until square wave with increased distortion. This increased

THD and heightened lower order harmonics will increase the filter size and cost. The benefits gained by linear control especially in closed loop systems over weights this additional burden due the filter size.

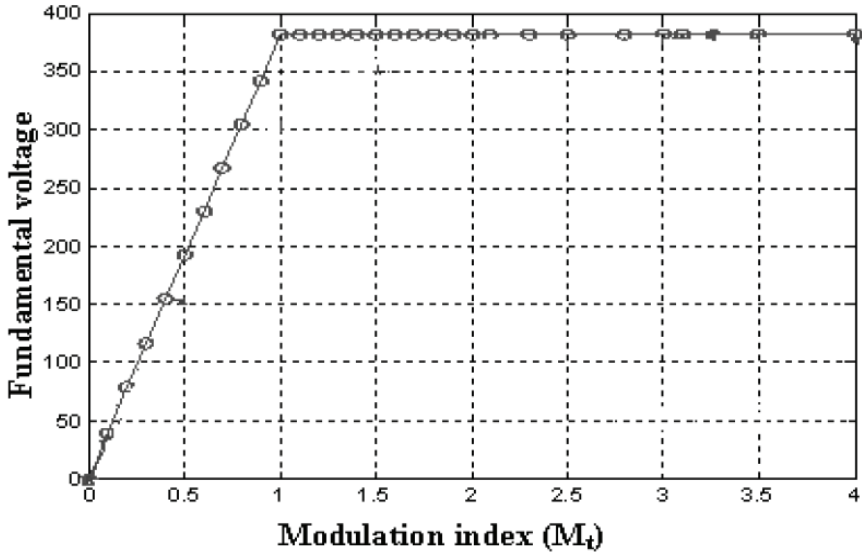


Fig. 8 – Fundamental voltage vs. M_1 – AMTCPWM.

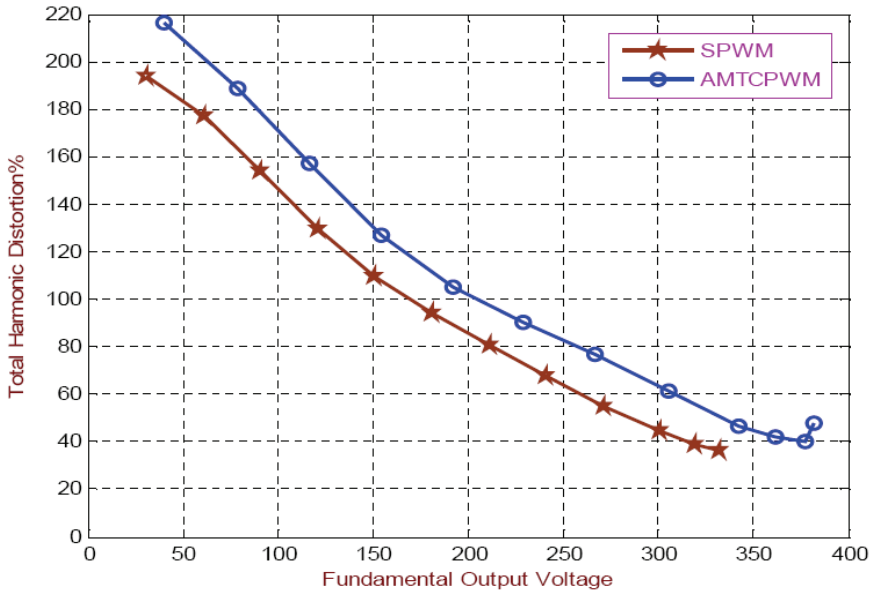


Fig. 9 – Fundamental voltage vs. THD – AMTCPWM.

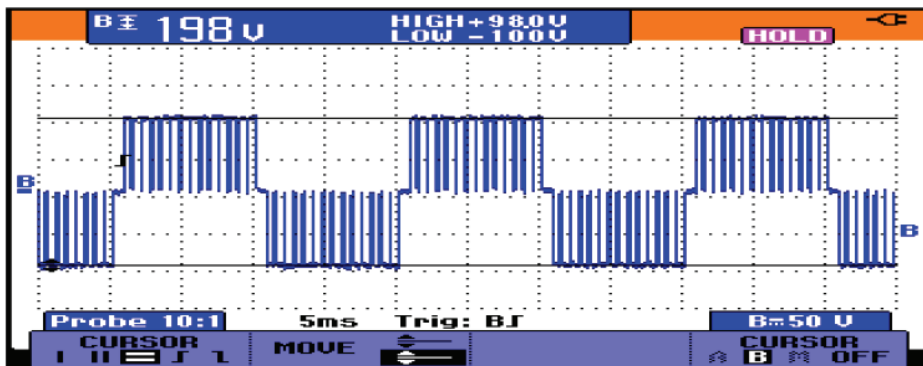
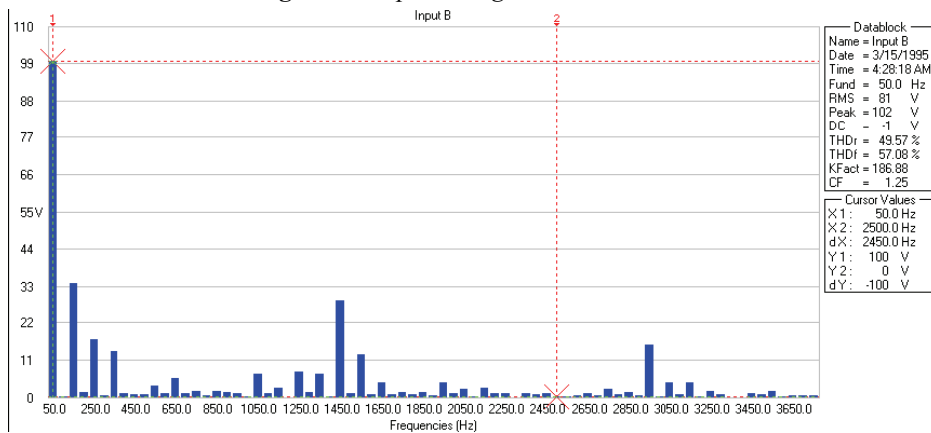
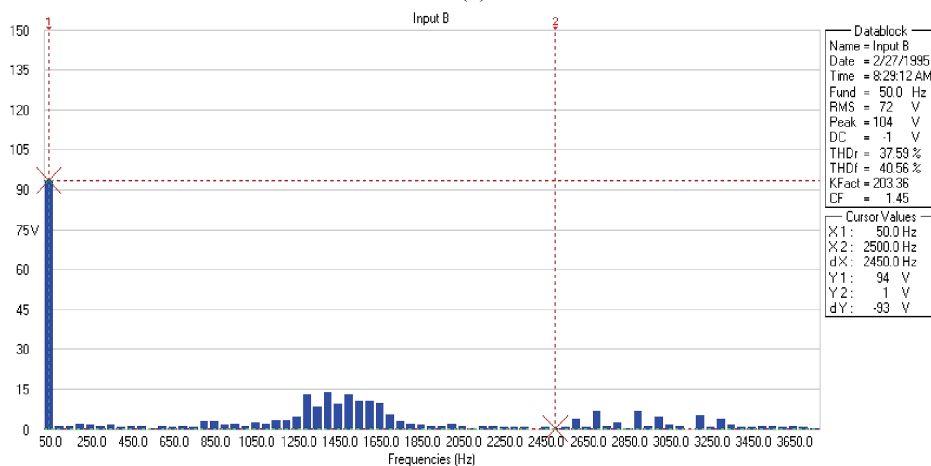


Fig. 10 – Output voltage – AMTCPWM.



(a)



(b)

Fig. 11 – Frequency spectrum: (a) SPWM; (b) AMTCPWM.

For proof-of-concept, a single-phase inverter is assembled and tested with a non-inductive resistor load ($R = 50 \Omega$). The input dc source is obtained by using single-phase diode rectifiers and capacitive filter and the V_{dc} is set to 100V. A Texas Instruments digital signal processor (DSP) TMS320F2407 is employed to generate gate control signals for the switches. Fig. 10 shows typical representative testing waveforms when the inverter is programmed using AMTCPWM technique ($M_t = 0.8$ and $M_f = 15$). Fig. 11a shows the frequency spectrum of SPWM ($M_a = 1$) while Fig. 11(b) shows the same for AMPTCPWM ($M_t = 0.8$).

5 Conclusion

The voltage linearity, harmonic distortion, and overmodulation range performance characteristics of a modulator are mainly dependent on the voltage-utilization level, i.e., modulation index. The linear voltage range of a PWM-VSI drive is mainly determined by the modulator characteristics. Effectual utilization of dc link voltage in PWM inverters through overmodulation causes nonlinearity in the feed forward channel. The proposed AMTCPWM technique provides full utilization (up to square wave region) without any pulse dropping and mode changing. The AMTCPWM method retains voltage linearity up to the square range without the use of any gain compensation techniques, and demonstrates betterments at higher output voltage ranges. The AMTCPWM method has the suitability of usage in closed loop systems. Though the worsened spectrum of AMTCPWM leads to bulky filtering, the proportionate variation of harmonic frequencies with the depth of modulation will ease the filter design.

6 Reference

- [1] K. Udhayakumar, P. Lakshmi, K. Boobal: Hybrid Posicast Controller for a DC-DC Buck Converter, Serbian Journal of Electrical Engineering, Vol. 5, No. 1, May 2008, pp. 121 – 138.
- [2] I. Batarseh: Power Electronic Circuits, John Wiley & Sons, New Jersey, 2004.
- [3] S. Jeevananthan, R. Nandhakumar, P. Dananjayan: Inverted Sine Carrier for Fundamental Fortification in PWM Inverters and FPGA Based Implementations, Serbian Journal of Electrical Engineering, Vol. 4, No. 2, Nov. 2007, pp. 171 – 187.
- [4] S. Bolognani, M. Zigliotti: Novel Digital Continuous Control of SVM Inverters in the Overmodulation Range, Applied Power Electronics Conference and Exposition APEC '96, March 1996, Vol. 1, pp. 219 – 223.
- [5] V. Jegathesan, J. Jerome: Non-traditional Method-based Solution for Elimination of Lower Order Harmonics in Voltage Source Inverter Feeding an Induction Motor Drive, Serbian Journal of Electrical Engineering, Vol. 5, No. 2, Nov. 2008, 273 – 283.

- [6] M. Bounadja, A. Mellakhi, B. Belmadani: A High Performance PWM Inverter Voltage-Fed Induction Machines Drive with an Alternative Strategy for Speed Control, *Serbian Journal of Electrical Engineering*, Vol. 4, No. 1, June 2007, 35 – 49.
- [7] M.A. Boost, P.D. Ziogas: 1998. State-of-the-art Carrier PWM Techniques: A Critical Evaluation, *IEEE Transactions on Industry Applications*, Vol. 24, No. 2, Mar/Apr 1988, pp. 271 – 280.
- [8] G. Giovanni, T.G. Habetler, F. Profumo, M. Pastorelli: 1993. Performance Evaluation of a Direct Torque Controlled Drive in the Continuous PWM-square Wave Transition Region, *IEEE Transactions on Power Electronics*, Vol. 10, No. 4, July 1995, pp. 464 – 471.
- [9] A.M. Hava, R.J. Kerkman, T.A. Lipo: Carrier-based PWM-VSI Overmodulation Strategies: Analysis, Comparison, and Design. *IEEE Transactions on Power Electronics*, Vol. 13, No. 4, July 1998, pp. 674 – 689.
- [10] J. Holtz, W. Lotzkat, A. Khambadkone: On Continuous Control of PWM Inverters in the Overmodulation Range Including the Six-step Mode, *IEEE Transactions on Power Electronics*, Vol. 8, No. 4, July 1993, pp. 546 – 553.
- [11] J.A. Houldsworth, P.A. Grant 1984, The Use of Harmonic Distortion to Increase the Output Voltage of a Three-phase PWM Inverter, *IEEE Transactions on Industry Applications*, Vol. IA- 20, No. 5, Sept. 1984, pp 1224 – 1228.
- [12] S. Jeevananthan, P. Dananjayan, S. Venkatesan: A Novel Modified Carrier PWM Switching Strategy for Single-phase Full-bridge Inverter, *Iranian Journal of Electrical and Computer Engineering*, Vol. 4, No. 2, Summer-Fall 2005, pp. 101 – 108.
- [13] R.J. Kerkman, T.M. Rowan, D. Leggate, B.J. Seibel: Control of PWM Voltage Inverters in the Pulse Dropping Region, *IEEE Transactions on Power Electronics*, Vol. 10, No. 5, Sep. 1995, pp. 559 – 565.
- [14] N. Mohan, T.M. Undeland, W.P. Robbins: *Power Electronics: Converters, Applications and Design*, John Wiley & Sons, 2002.
- [15] T.M. Rowan, R.J. Kerkman, T.A. Lipo: Operation of Naturally Sampled Current Regulators in the Transition Mode, *IEEE Transactions on Industry Applications*, Vol. IA- 23, No. 4, July 1987, pp 586 – 596.
- [16] A. Schonung, H. Stemmler: Static Frequency Changers with Subharmonic Control in Conjunction with Reversible Variable Speed AC Drives, *Brown Boveri Review*, Vol. 51, No. 8/9, Aug./Sep. 1964, pp 555 – 577.
- [17] H.W. van der Broeck, H.C. Skudelny, G.V. Stanke: Analysis and Realization of a Pulse Width Modulator based on Voltage Space Vectors, *IEEE Transaction on Industry application*, Vol. 24, No. 1, Part 1, Jan/Feb 1988, pp. 142 – 150.
- [18] K. Kaura, V. Blasko: A New Method to Extend Linearity of a Sinusoidal PWM in the Overmodulation Region, *IEEE Transaction on Industry Applications*, Vol. 32, No. 5, Sep./Oct. 1996, pp. 1115 – 1121.
- [19] S. Jeevananthan, P. Dananjayan: Static Model Verification of IRF Power MOSFETs using Fluke Temperature Probe (80T-150U) and Performance Comparison of TEHPWM Methods, *International Conference on Power Electronics and Drive Systems (PEDS2005)*, Kuala Lumpur, Malaysia, Nov. 28 – Dec. 1 2005, Vol. 1, pp. 681 – 686.